Coupling strength of the $N^*(1535)S_{11}$ to the $K^+\Lambda$ channel

T. Mart

Departemen Fisika, FMIPA, Universitas Indonesia, Depok 16424, Indonesia

(Dated: March 28, 2013)

Abstract

The $N^*(1535)S_{11}$ coupling strength to the $K^+\Lambda$ channel, $g_{N^*(1535)\Lambda K^+}$, is extracted from the latest and largest $K^+\Lambda$ photoproduction database by using an isobar model. It is found that the coupling is small. In term of the coupling ratio the best result is $R \equiv |g_{N^*(1535)\Lambda K^+}/g_{N^*(1535)\eta p}| = 0.460 \pm 0.172$, much smaller than that obtained from the isobar analysis of the J/ψ decays, i.e., 1.3 ± 0.3, but consistent with the results of the unitary chiral approach of the same decay processes as well as the partial wave analysis of kaon photoproduction, i.e., $R = 0.5 \sim 0.7$. The different results of R found here and in literature to date suggest that a more solid definition of the coupling constant, especially in the case of $N^*(1535)S_{11}$ state, is urgently required, before a fair comparison can be made.

PACS numbers: 13.60.Le, 25.20.Lj, 14.20.Gk

The nucleon resonance $N^*(1535)S_{11}$ occupies a special place in the Particle Data Group (PDG) listing, because it has an extraordinarily large branching fraction to the ηN channel, i.e., 45−60% [1]. To explain this a number of mechanism has been proposed, e.g., the $K\Lambda$-$K\Sigma$ [2] and meson-baryon [3] quasi-bound states, as well as the introduction of pentaquark component in the nucleon besides the conventional uud state [4]. At the quark level, the existence of the $N^*(1535)S_{11}$ leads to a long standing problem, since the conventional constituent quark model predicts this resonance to be the lowest mass state [5], in contrast to the fact that there exists an $N^*(1440)P_{11}$ state with $J^p = 1/2^+$ as listed in the Review of Particle Physics by PDG [1]. A suggested solution to this mass reverse problem is the introduction of the pentaquark admixture [4]. However, such mechanism leads to a large $N^*(1535)S_{11}$ coupling to the $K\Lambda$ channel. More dramatically, by analyzing the $J/\psi \to \bar{p}K^+\Lambda$ and $J/\psi \to \bar{p}p\eta$ experimental data within an isobar model it was found that the coupling of the $N^*(1535)S_{11}$ to the $K\Lambda$ channel is larger than its coupling to the ηN channel, i.e., $R \equiv |g_{N^*(1535)\Lambda K^+}/g_{N^*(1535)\eta p}| = 1.3 \pm 0.3$ [6]. A direct consequence of this large ratio is that the mass and width of the $N^*(1535)S_{11}$ should be 1400 and 270 MeV, respectively. Clearly, this is an unexpected result, since this finding is considered [7] to differ radically from the standard value [1]. However, we observe that in literature the values of this ratio are wildly scattered. For instance, the unitary chiral approach found $R = 0.5 \sim 0.7$ [8]. A similar result was obtained by the partial wave analysis of kaon photoproduction [9], whereas a coupled-channels calculation predicted $R = 0.8 \sim 2.6$ [8, 10]. On the other hand, the result of the s-wave pion-nucleon scattering analysis in a unitarized chiral effective Lagrangian indicates that $|g_{N^*(1535)\Lambda K^+}|^2 > |g_{N^*(1535)\eta p}|^2$ [11]. It is important to note that these different results originate from different methods of analysis as well as different data and, as a consequence, there exist conceptual differences between the extracted coupling constant. Therefore, care must be taken when one wants to compare these results in term of a unique definition of coupling constant.

With the accumulating precise kaon photoproduction data from the modern continues electron beam facilities such as CEBAF, ELSA, SPring-8, ESRF, and MAMI, it is obviously important to consider the $\gamma p \to K^+\Lambda$ process for extracting the $g_{N^*(1535)\Lambda K^+}$ coupling, since the $g_{N^*(1535)\eta p}$ coupling is relatively well known [1]. The process has been studied for decades by using a number of phenomenological models. However, the isobar model is the most relevant one for the present discussion. We note that most of the models did not include

the $N^*(1535)S_{11}$ resonance because its mass is located below the reaction threshold. Other models include this resonance mainly because kaon photoproduction is one of the coupled channels being analyzed. Interestingly, the conclusions from these kaon photoproduction studies vary from one analysis to another. For instance, Refs. [12, 13] found that the resonance is less important in the $K^+\Lambda$ photoproduction, whereas Refs. [14, 15] drew an opposite conclusion.

Given the critical consequence of large R in many aspects of hadronic physics, we believe that it is urgent to extract the value from kaon photoproduction data. In this paper we report on the result of this extraction, which makes use of an isobar model constructed from appropriate Feynman diagrams based on our previous but latest model [16]. The model consists of the standard s-, u-, and t-channel Born terms along with the $K^{*+}(892)$, $K_1(1270)$ vector mesons and the $\Lambda^*(1800)S_{01}$, $\Lambda^*(1810)P_{01}$ hyperon resonance. In the s-channel the model takes the $N^*(1650)S_{11}$, $N^*(1700)D_{13}$, $N^*(1710)P_{11}$, $N^*(1720)P_{13}$, $N^*(1840)P_{11}$, $N^*(1900)P_{13}$, $N^*(2080)D_{13}$, $N^*(2090)S_{11}$, and $N^*(2100)P_{11}$ nucleon resonances into account. Note that the choice of these nucleon resonances is consistent with the result of the partial wave analysis [9] and the 2012 PDG listing [1]. We have also compared our resonance configuration with that used by the Ghent group [17] and found that our configuration is consistent up to spin 5/2 resonances. The omission of spin 5/2 resonances in our model was discussed in Ref. [16].

To approximately account for unitarity corrections at tree-level we use energy-dependent widths along with partial branching fractions in the resonance propagators [18]. Furthermore, to account for the fact that hadrons are composite objects, hadronic form factors are considered in hadronic vertices, where the gauge invariance of the amplitude after the form factor inclusion is restored by using the Haberzettl prescription [19]. The model fits all latest $K^+\Lambda$ photoproduction data consisting of differential cross section [20–23], recoil polarization [20, 24], beam-recoil double polarization [25, 26] as well as photon Σ and target T asymmetries [24] data. In total, our database consists of more than 3500 data points. To our knowledge, this is the largest $K^+\Lambda$ photoproduction database intended for the present purpose. Two different models (A and B) were proposed in Ref. [16]. Both models use the same resonance configuration as described above, but in the model A [B] the mass and width of the $N^*(2080)D_{13}$ [$N^*(1900)P_{13}$] resonance were considered as free parameters. As a result a total χ^2 of 9084 (9494) was obtained in model A (B). For a more detailed discussion on

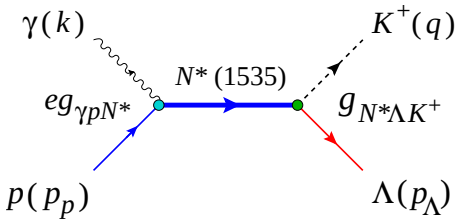

FIG. 1: (Color online) Contribution of the $N^*(1535)S_{11}$ diagram to the kaon photoproduction process.

the performance of both models we refer the reader to Ref. [16].

In the present work we include the $N^*(1535)S_{11}$ contribution in both models and refit the experimental data to the model calculations by adjusting all coupling strengths. The Lagrangian for the magnetic transition of this resonance reads [27]

$$\mathcal{L}_{\gamma NN^*} = \frac{e}{4m_N}\bar{\psi}_{N^*} g_{\gamma NN^*}\gamma_5\sigma_{\mu\nu}\,\psi_N\,F^{\mu\nu} + \text{H.c.}, \tag{1}$$

where $F^{\mu\nu} = \partial^\mu A^\nu - \partial^\nu A^\mu$ and other terms are self explaining. In the $K\Lambda N^*$ vertex one obtains [6]

$$\mathcal{L}_{N^*\Lambda K} = -ig_{N^*\Lambda K}\bar{\psi}_\Lambda\Phi_K\,\psi_{N^*} + \text{H.c.}. \tag{2}$$

The corresponding Feynman diagram is depicted in Fig. 1. Obviously, only the product of $g_{\gamma pN^*}\,g_{N^*\Lambda K}$ can be extracted from the fitting process. Nevertheless, the $g_{\gamma pN^*}$ coupling is relatively well known from the PDG value of the helicity amplitude. For a negative-parity spin 1/2 resonance this amplitude can be related to the electromagnetic coupling constant via [27]

$$A^p_{1/2} \;=\; \frac{1}{2m_p}\left(\frac{m^2_{N^*}-m^2_p}{2m_p}\right)^{1/2}\; eg_{\gamma pN^*}\;. \tag{3}$$

Using $A^p_{1/2} = 0.090 \pm 0.030$ GeV$^{-1/2}$ [1] we obtain $g_{\gamma pN^*} = 0.335 \pm 0.112$.

The photoproduction amplitude $\mathcal{M}$ is conventionally decomposed into the gauge- and Lorentz-invariant matrices M_i,

$$\mathcal{M} = \sum_{i=1}^{4} A_i(s,t,u)\,M_i\;, \tag{4}$$

where s, t, and u are Mandelstam variables, since all observables can be calculated from A_i. The explicit forms of A_i and M_i can be found, e.g., in Ref. [18]. Note that, in the present

TABLE I: The $N^*(1535)S_{11}$ coupling constant $g_{N^*\Lambda K^+}$, the hadronic form factor cut-off Λ, and the coupling constant ratio R obtained from three different models in the present work. The product of electromagnetic and hadronic couplings $g_{\gamma pN^*}\, g_{N^*\Lambda K^+}$ is obtained from refitting the experimental data. Also shown in this Table are the number of free parameters ($N_{\rm par.}$), the χ^2, and the χ^2 per number of degrees of freedom ($\chi^2/N_{\rm dof}$) for each model.

Parameter	A1	A2	B1
$g_{\gamma pN^*}\, g_{N^*\Lambda K^+}$	0.220 ± 0.033	0.286 ± 0.030	0.157 ± 0.024
$g_{N^*\Lambda K^+}$	0.656 ± 0.240	0.853 ± 0.298	0.469 ± 0.172
R	0.354 ± 0.138	0.460 ± 0.172	0.253 ± 0.099
$\Lambda_{\rm Born}$ (GeV)	0.920	1.070	0.483
$\Lambda_{\rm Res.}$ (GeV)	1.356	1.364	1.460
$N_{\rm par.}$	30	31	30
χ^2	9035	8716	9480
$\chi^2/N_{\rm dof}$	2.555	2.466	2.681

paper models A1 and B1 refer to the two original models A and B explained above [16] but after including the $N^*(1535)S_{11}$ resonance in the model and refitting the experimental data. Recently, we found that by adding a $\Lambda^*(1600)P_{01}$ hyperon resonance in the original model A significant improvement can be achieved, i.e., the χ^2 is greatly reduced and the background form factor cut-off is increased [28]. In the present study we find that including the $\Lambda^*(1600)P_{01}$ in the original model A reduces the χ^2 from 9084 to 8817. By adding the $N^*(1535)S_{11}$ to this result we obtain model A2 which has $\chi^2 = 8716$ as listed in Table I. As seen in this Table, the inclusion of the $\Lambda^*(1600)P_{01}$ simultaneously increases the Born cut-off, whereas the resonance one seems to be unaffected.

The problem of the over-damped Born terms due to the extremely soft (small) Born cut off has been extensively discussed in literature (see e.g. Ref. [29]). It was suspected that such a cut-off is artificial and the corresponding model is, therefore, far from a realistic description of the process [30]. This problem seems to appear in model B1, for which the value of $\Lambda_{\rm Born}$ is less than one half of that obtained in model A2.

We note that there is a strong correlation between the $N^*(1535)S_{11}$ and $N^*(1650)S_{11}$

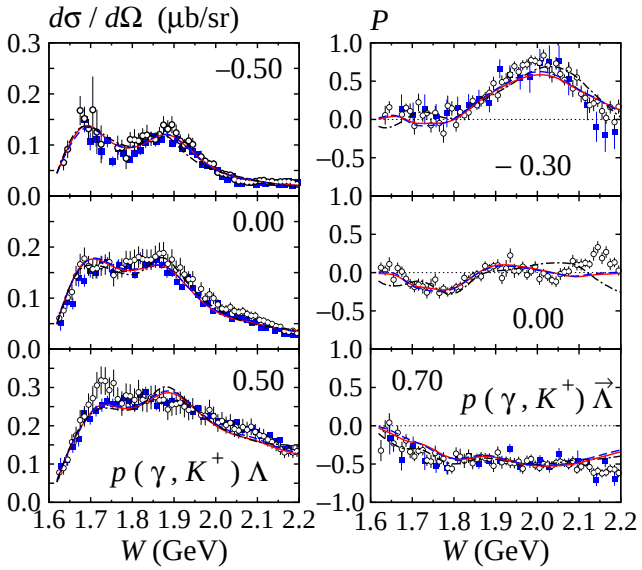

FIG. 2: (Color online) Differential cross sections $d\sigma/d\Omega$ and recoil polarization observables P sampled at three different kaon angles θ for the three models given in Table I. The value of $\cos\theta$ is given in each panel. The solid, dashed, and dash-dotted lines correspond to the models A1, A2, and B1, respectively. Experimental data are from the CLAS collaboration (solid squares [20] and open circles [21]).

resonances. This is indicated by the large value of the correlation coefficient of these resonances given by the Minuit output (e.g., about 0.94 for model A2). Nevertheless, we found that the extracted couplings of both resonances are comparably small.

The performance of the presented models in describing the selected experimental data is displayed in Figs. 2 and 3. Obviously, models A1 and A2 are superior to model B1. Although the difference between models A1 and A2 in the differential cross section and recoil polarization data is graphically subtle, we find that numerically the presence of the $\Lambda^*(1600)P_{01}$ in model A2 improves the agreement with data. Sizable improvements are also found in the double polarization observables as well as in the target and photon asymmetries. Furthermore, from Table I we can conclude that model A2 is the most reliable model for our present purpose.

The presence of the $N^*(1535)S_{11}$ in model A1, A2, and B1 improves the χ^2 from 9084 to 9035, from 8817 to 8716, and from 9494 to 9480, respectively. Therefore, the presence of the $N^*(1535)S_{11}$ has the strongest effect in model A2. This effect is closely related to the

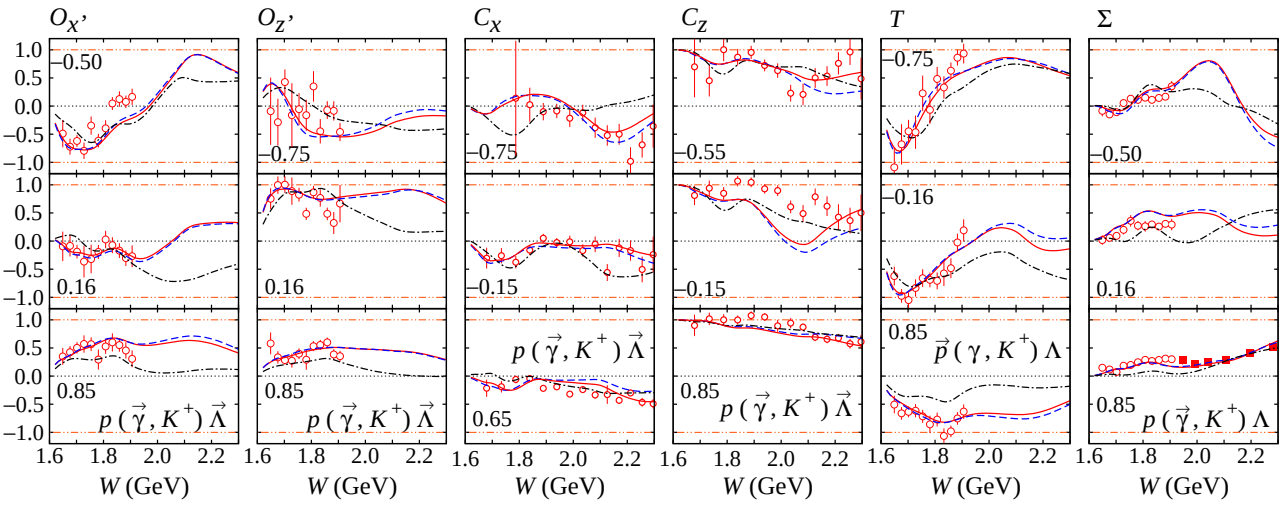

FIG. 3: (Color online) Same as Fig. 2, but for the beam-recoil double polarization observables $O_{x'}$, $O_{z'}$, C_x, and C_z, as well as the target T and beam Σ asymmetries. The notation of the curves is as in Fig. 2. Experimental data are from the GRAAL [24, 25], CLAS [26], and LEPS collaborations [22].

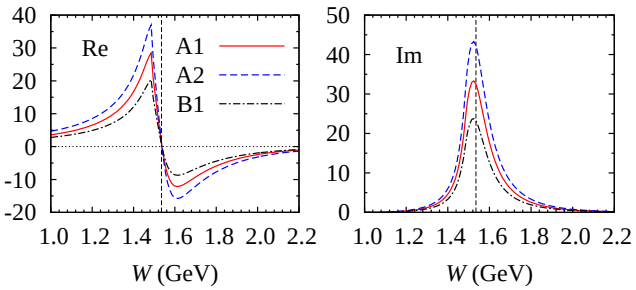

FIG. 4: (Color online) Real and imaginary parts of the A_1 amplitude (in 10^{-3} GeV^{-2}) obtained from three different models.

$N^*(1535)S_{11}$ coupling strength given in Table I. Since the contribution of this resonance to the A_i in Eq. (4) is $A_2 = 0$, and $A_3 = A4 \propto A_1$, information on the A_1 displayed in Fig. 4 is sufficient for estimating the $N^*(1535)S_{11}$ effect. The different magnitudes of A_1 exhibited by the three models in Fig. 4 originates from the different $g_{N^*\Lambda K^+}$ magnitudes shown in Table I. Thus the larger the $g_{N^*\Lambda K^+}$ value, the more important the contribution of this resonance to the photoproduction process.

Although the strongest effect of the $N^*(1535)S_{11}$ appears in model A2, comparison of

the $N^*(1535)S_{11}$ contribution with those from other dominant resonances in this model is extremely important, especially when we consider the claim that the $N^*(1535)S_{11}$ dominates the $pp \to pK^+\Lambda$ reaction [6], whereas the experimental Dalitz plot strongly suggests the $N^*(1650)S_{11}$ as a dominant resonance at low energies [31]. The comparison is given in Fig. 5. Obviously, the dominant contributors near threshold are the $N^*(1650)S_{11}$ and $N^*(1720)P_{13}$ resonances. Compared with these two resonances the $N^*(1535)S_{11}$ contribution is significantly smaller. This result corroborates the finding of previous studies using isobar model [12, 32] and is in agreement with the result of the Dalitz plot [31].

To obtain the ratio R given in Table I we need to calculate the $g_{N^*(1535)\eta p}$ coupling constant. Using the branching ratio given by PDG, i.e., $\Gamma(N\eta)/\Gamma_{\rm total} = 0.42 \pm 0.10$ [1] and the relation between the branching ratio and the corresponding coupling constant [27]

$$\Gamma_{N^*} = \frac{g^2_{N^*\eta N}}{4\pi}\, p\, \frac{E_N + m_N}{\sqrt{s}}, \tag{5}$$

where $p = [\{s-(m_N+m_\eta)^2\}\{s-(m_N-m_\eta)^2\}]^{1/2}/2s^{1/2}$ and $E_N = (p^2+m_N^2)^{1/2}$, we obtain $|g_{N^*(1535)\eta p}| = 1.853 \pm 0.244$, which is in good agreement with the result obtained in Ref. [8]. Using this value and the extracted $g_{N^*\Lambda K^+}$ from kaon photoproduction we obtain the ratio R for all three models and list them in Table I. Since model A2 has been shown to be the

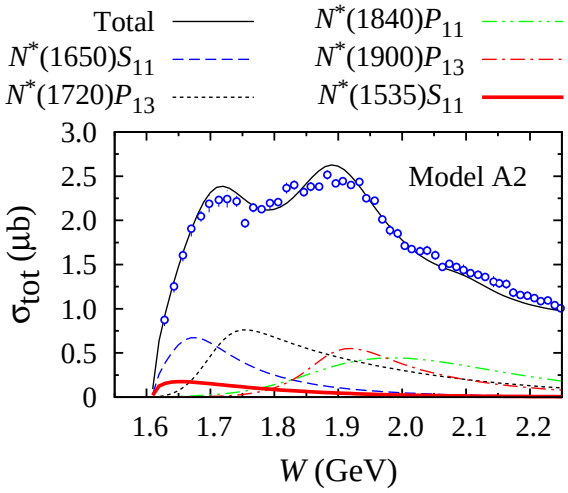

FIG. 5: (Color online) Contributions of the most important resonances to the total cross section of the $\gamma p \to K^+\Lambda$ process for Model A2.

most reliable model, we believe that the best result of the present work yields

$$R = 0.460 \pm 0.172. \tag{6}$$

Note that the large error bar is mainly due to the large uncertainties in the PDG values of the $A_{1/2}$ and $\Gamma(N\eta)/\Gamma_{\rm total}$ [1] (see also Table I for the error given by the fit to kaon photoproduction data). This result is obviously smaller than that obtained in Ref. [6], i.e., 1.3 ± 0.3, and slightly below the lower bound of the coupled-channels result, i.e. $0.8 \sim 2.6$ [8, 10]. However, the present result is consistent with the results from the unitary chiral approach of the J/ψ decays [8] and the partial wave analysis of kaon photoproduction, i.e., $R = 0.5 \sim 0.7$. We also note that the product of $g_{\gamma pN^*} g_{N^*\Lambda K^+}$ extracted from the $K^+\Lambda$ photoproduction in a recent isobar analysis [12] is even smaller than the present result (see Table II of Ref. [12]). Very likely the smaller value in Ref. [12] is due to the complication of various interfering resonances (about 23 nucleon and hyperon resonances) in the model. To understand the different values obtained from the unitary chiral approach [8] and the isobar model [6], the former was interpreted as a measure of the strength of the $K\Lambda$ component in the $N^*(1535)S_{11}$ wave function, whereas the latter was considered as the fitted coupling strength near the $K\Lambda$ threshold [8]. The result of the present isobar model given in Eq. (6) supports the small value of the $g_{N^*(1535)\Lambda K^+}$. Nevertheless, as stated above, a more conclusive result should wait for a more solid definition of the resonance coupling constant, since there exist conceptual differences in current and available extracted coupling constants. We note, however, that one of the possible solutions to this problem is the introduction of the residue of the transition amplitude as explained in the Review of the N and Δ Resonances of the 2012 Review of Particle Physics [1]. In principle, this residue can be calculated from a contour integral of the transition amplitude around the pole position in the complex energy plane and the result is proportional to the coupling constant. Thus, future extractions of the hadronic coupling constants should consider this issue in a comprehensive way, i.e., it applies not only to the $g_{N^*(1535)\Lambda K^+}$ coupling, but also to both $g_{\gamma pN^*}$ and $g_{N^*(1535)\eta p}$ couplings used to derive R.

In conclusion, we have extracted the $g_{N^*(1535)\Lambda K^+}$ coupling strength and its ratio to the $g_{N^*(1535)\eta p}$ coupling from a large $K^+\Lambda$ photoproduction database by means of an isobar model. The result is significantly smaller than that obtained from the isobar analysis of J/ψ decays, but comparable to the results of the unitary chiral calculation as well as the

partial wave analysis. We have indicated that the result is not conclusive due to the inherent problem in the method.

The author thanks Bing Song Zou for encouraging this study. This work has been supported in part by the University of Indonesia and by the Competence Grant of the Indonesian Ministry of Education and Culture.

---

[1] J. Beringer *et al.* [Particle Data Group], Phys. Rev. D **86**, 010001 (2012).

[2] N. Kaiser, P. B. Siegel, and W. Weise, Phys. Lett. B **362**, 23 (1995).

[3] T. Inoue, E. Oset, and M. J. Vicente Vacas, Phys. Rev. C **65**, 035204 (2002).

[4] B. S. Zou, Nucl. Phys. A **835**, 199 (2010).

[5] S. Capstick and W. Roberts, Phys. Rev. D **58**, 074011 (1998).

[6] B. C. Liu and B. S. Zou, Phys. Rev. Lett. **96**, 042002 (2006)

[7] A. Sibirtsev, J. Haidenbauer, and Ulf-G. Meißner, Phys. Rev. Lett. **98**, 039101 (2007).

[8] L. S. Geng, E. Oset, B. S. Zou, and M. Döring, Phys. Rev. C **79**, 025203 (2009).

[9] A. V. Sarantsev, V. A. Nikonov, A. V. Anisovich, E. Klempt and U. Thoma, Eur. Phys. J. A **25**, 441 (2005).

[10] G. Penner and U. Mosel, Phys. Rev. C **66**, 055212 (2002).

[11] P. C. Bruns, M. Mai and U. G. Meissner, Phys. Lett. B **697**, 254 (2011).

[12] O. V. Maxwell, Phys. Rev. C **85**, 034611 (2012).

[13] W. T. Chiang, B. Saghai, F. Tabakin, and T.-S. H. Lee, Phys. Rev. C **69**, 065208 (2004); Phys. Lett. B **517**, 101 (2001).

[14] B. Julia-Diaz, B. Saghai, T. S. H. Lee and F. Tabakin, Phys. Rev. C **73**, 055204 (2006).

[15] V. Shklyar, H. Lenske, and U. Mosel, Phys. Rev. C **72**, 015210 (2005).

[16] T. Mart and M. J. Kholili, Phys. Rev. C **86**, 022201(R) (2012).

[17] L. De Cruz, T. Vrancx, P. Vancraeyveld, and J. Ryckebusch, Phys. Rev. Lett. **108**, 182002 (2012).

[18] F. X. Lee, T. Mart, C. Bennhold, H. Haberzettl, and L. E. Wright, Nucl. Phys. A **695**, 237 (2001).

[19] H. Haberzettl, C. Bennhold, T. Mart and T. Feuster, Phys. Rev. C **58**, R40 (1998).

[20] R. Bradford *et al.*, Phys. Rev. C **73**, 035202 (2006).

[21] M. E. McCracken *et al.*, Phys. Rev. C **81**, 025201 (2010).

[22] M. Sumihama *et al.*, Phys. Rev. C **73**, 035214 (2006).

[23] K. Hicks *et al.*, Phys. Rev. C **76**, 042201 (2007).

[24] A. Lleres *et al.*, Eur. Phys. J. A **31**, 79 (2007).

[25] A. Lleres *et al.*, Eur. Phys. J. A **39**, 146 (2009).

[26] R. Bradford *et al.*, Phys. Rev. C **75**, 035205 (2007).

[27] T. Feuster and U. Mosel, Phys. Rev. C **59**, 460 (1999).

[28] T. Mart and N. Nurhadiansyah, Few-Body Syst. 2013, DOI: 10.1007/s00601-012-0497-9.

[29] P. Bydžovský and T. Mart, Phys. Rev. C **76**, 065202 (2007).

[30] T. Mart and C. Bennhold, Phys. Rev. C **61**, 012201(R) (1999).

[31] S. Abd El-Samad *et al.*, Phys. Lett. B 688, 142 (2010).

[32] T. Mart and A. Sulaksono, Phys. Rev. C **74**, 055203 (2006); T. Mart, Phys. Rev. C **82**, 025209 (2010).